HEAT TREATMENTS OF WELD ALLOY 625: INFLUENCE ON THE

MICROSTRUCTURE, MECHANICAL PROPERTIES AND CORROSION RESISTANCE

François Cortial, Jean-Michel Corrieu, Chantal Vernot-Loier

Centre d'Etudes des Structures et des Matériaux Navals
DGA/DCN INDRET
44620 LA MONTAGNE - FRANCE

Abstract

The effects of heat treatments of the industrial type: 8 h hold times at temperatures comprised between 600°C and 1000°C, on the structural, mechanical and corrosion resistance characteristics of weld alloy 625 have been studied. During the heat treatments, the mean concentration ratios of Nb, Mo, Si, Cr, Ni and Fe elements between the interdendritic spaces and dendrite cores feature but little evolution up to 850°C. Beyond that temperature, this ratio approximates 1 and the composition heterogeneity has practically disappeared at 1000°C. A 8 h heat treatment at temperatures comprised between 650°C and 750°C results in increased mechanical strength values and reduced ductility and impact strength linked to the precipitation of body-centred tetragonal intermetallic γ'' Ni_3Nb phase in the interdendritic spaces. A 8 h treatment in the temperature range comprised between 750°C and 950°C has catastrophic effects on all mechanical characteristics in relation with the precipitation, in the interdendritric spaces, of the stable orthorhombic intermetallic δ $Ni_3(Nb, Mo, Cr, Fe, Ti)$ phase. At 1000°C, the ductility and impact strength are restored. However, the higher the heat treatment temperature, the weaker the mechanical strength. Heat treatments have no effect on the pitting resistance of weld alloy 625 in sea-water. The comparison of the results of this study on weld alloy 625 with those previously obtained on forged metal 625 shows that heat treatments below 650°C and above 1000°C are the sole treatments allowing to avoid embrittlement and impairment of the corrosion resistance characteristics of alloy 625.

Introduction

Alloy 625 features good mechanical strength, combined with good corrosion resistance and good weldability characteristics. It can be used for welding low alloyed steels or high yield strength steels with alloy 625 for repairing these steels by welding or by coating process in order to protect them from corrosion. In such cases, post-welding heat treatments are necessary to preserve the characteristics of the heat affected zone (HAZ) of ferritic steels. As few data was avalaible on the evolution of the structure and properties of alloy 625 during industrial heat treatments (1-3), a first study was conducted on a forged bar (4) which has allowed determining the temperature ranges within which the different phase precipitations occur : intermetallic γ'' phase, carbides $M_{23}C_6$, M_6C, MC and establishing a link between the mechanical properties and corrosion resistance versus the microstructure of the wrought metal 625.
This paper presents the results obtained concerning the effects of industrial type heat treatments: 8 h hold times at temperatures comprised between 600°C and 1000°C and air cooling, on the microstructure, mechanical characteristics and corrosion resistance in sea-water and chloride environments of weld alloy 625.

Experimental Procedure

Material

Weld metal 625 used for the study originates from a weldment of 32 x 150 x 750 mm^3 obtained by automatic tungsten inert gas (TIG) welding process on an A533 steel plate of 90 x 230 x 940 mm^3. The essential welding parameters are given in Table I and the chemical compositions of the wire and deposited metal are given in Table II.

Height pieces size 170 x 65 x 30 mm^3 have been cut with their length parallel to the welding direction (Fig. 1a), the A533 steel area being eliminated by milling of the 8 pieces. The pieces (Table III) have been heat treated as follows: heating in 50°C increments per hour, 8 h hold time at the selected temperature, cooling in the air at a cooling rate of 900°C/h.

The test specimen sampling plan is identical for the different thermal states (Fig. 1b).

Structural investigations

Test specimens corresponding to all thermal states have been examined with an optical microscope under natural light and differential interferential contrast (DIC).

Both prior to and after the corrosion resistance tests, the test specimens have been examined with a scanning electron microscope (SEM) equipped with an X-ray energy dispersive spectrometer (X-EDS) to relate the attacks to the structure.
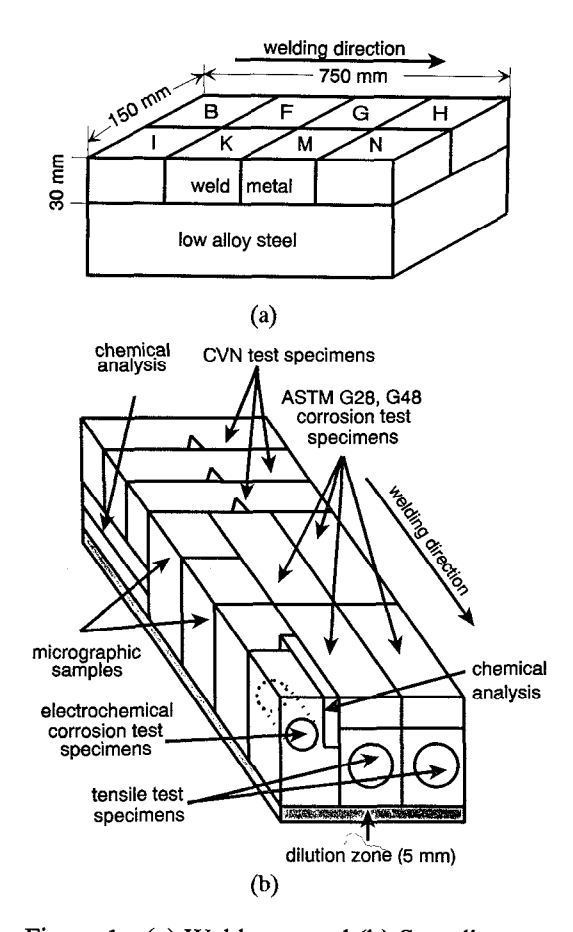

(a)

(b)

Figure 1 - (a) Weldment and (b) Sampling

Table I -Welding parameters

Wire dia. (mm)	Gas	Current (A)	Voltage (V)	Speed (cm.min^{-1})	Wire feed rate (m.min^{-1})
0.8	pur Ar	170 ± 5	13 ± 0.2	10 ± 0.2	2 ± 0.05

Table II - Chemical compositions (weight %)

Elements	C	Ni	Cr	Mo	Nb	Fe	Ti	Al	Si	Mn
Wire	0.042	61	22	9	3.55	3.60	0.26	0.27	0.13	0.10
Weld Metal (Lower)	0.041	59.7	21.9	8.90	3.50	5	0.27	0.25	0.12	0.12
Weld Metal (Upper)	0.041	60.6	22	8.90	3.50	3.90	0.27	0.25	0.12	0.10

Table III - Correspondence between identified pieces and heat treatment temperatures

Piece	B	F	G	H	I	K	M	N
Temperature	—	600° C	650° C	700° C	750° C	850° C	950° C	1000° C

The back-scattered electron atomic contrast images have been obtained at V= 15 kV, I = 7 nA. The evolution of the chemical compositions of dendrite cores and interdendritic spaces has been studied using both the X-EDS and an electron microprobe analyser at V=15kV and I=15 nA at a rate of 20 points of analysis selected within areas featuring maximum back-scattered electron contrasts.

For the thermal states corresponding to particularities of the mechanical behaviour or corrosion resistance characteristics, the microstructure has been studied on thin foils and extractive replicas on a transmission electron microscope (TEM) equipped with a double tilt holder and a horizontal X-EDS microanalyzer. The X-EDS analysis being performed using a horizontal microanalyzer, the thin foils are tilted by + 37° thus causing excitation of the copper clamping ring and the presence of copper peaks on the spectra. The weight compositions have been calculated using the k factors technique developed by Cliff and Lorimer (5).

Mechanical properties

The same mechanical tests have been performed for the different thermal states. Vickers hardness has been measured under a load of 10 kgf on micrographic test specimens. The yield strength (YS 0.2% offset), the ultimate tensile strength (UTS), the elongation (EL) and reduction of area (RA) have been determined at +20°C on proportional test specimens with the major axis parallel to the welding direction (Fig. 1b). The impact strength tests at +20°C have been made on CHARPY V-notch test specimens having their major axis perpendicular to the welding direction and the notches perpendicular to the skins (fig. 1b).

Corrosion

While the intergranular corrosion resistance test defined in ASTM standard G28 is only specified for wrought metals, this test has been used within the scope of the present study in order to compare the weld alloy 625 with the forged metal (4) and compare the different thermal states with each other. The test has been performed for each thermal state on test specimens size $70 \times 10 \times 3$ mm^3 sampled with their major axis parallel to the welding direction (Fig. 1b).

A corrosion pitting chemical test ASTM standard G 48 has been performed for each thermal state on test specimens size $70 \times 10 \times 3$ mm^3 sampled with their major axis parallel to the welding direction (Fig. 1b).

The electrochemical potentiokinetic reactivation method (6) has been performed. The test medium had been adjusted on wrought metal; it consisted of a solution containing 236 ml H_2SO_4 (d = 1.83), 58 mg NaCl and 400 ml H_2O. In the case of the weld metal, an aqueous solution titrated at 95% of the previous one, held at a temperature of 30°C, and deoxygenated by purified nitrogen (N50) bubbling process was used. The electrochemical paremeters were the following : 120 sec. hold time at corrosion potential, sweep toward electropositive potentials at 2 mV.s^{-1} up to 600 mV/ECS, 240 sec. hold time at + 600 mV/ECS, sweep toward electronegative potentials at 2mV.s^{-1} down to - 200 mV/ECS.

The electrochemical behaviour of the materials has been characterized in 30 g.l^{-1} NaCl medium. The test specimens were inserted in a teflon fixture, and mounted on a rotating disc electrode. The rotation speed was 1000 rev.min^{-1}. The potientiokinetic curves were plotted from - 0.4 to + 1.2 V/ECS, at a sweeping rate of 0.07 mV.s^{-1}.
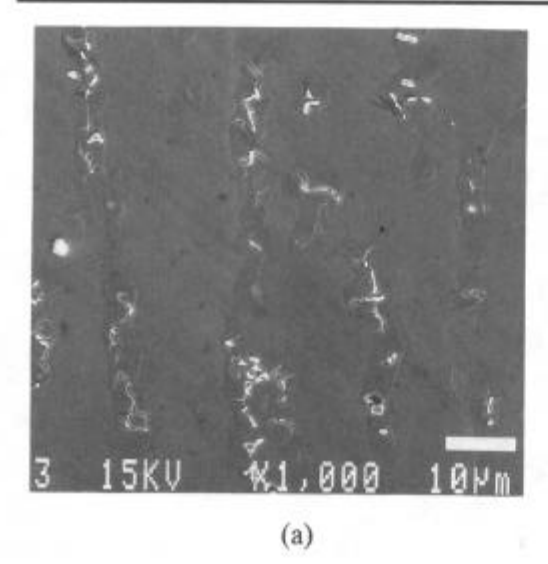
Results

Structural changes

The structure of the weld metal in rough-welding condition is shown on figure 2. The dendrite network in dark clearly appears in back-scattered electrons due to the segregation of heavy elements Nb and Mo in the interdendritic spaces which appear in a lighter tone. The results of composition analysis made with the electron microprobe on the dendrite cores and interdendritic spaces of the rough welded metal are presented in table IV. They show that elements Mo, Si and, more particularly Nb, are rejected in the interdendritic liquid during the solidification process, Ni and Fe being concentrated in the dendrite cores (7-9). As far as it is concerned, Cr does not appear to segregate contrarily to what has been observed on an earlier study of a TIG weldment (9).

Table IV - Electron microprobe analysis obtained on dendrite cores and interdendritic spaces of the rough-welded alloy (weight %)

Analyzed areas		Ni	Cr	Mo	Nb	Fe	Si
	Min	60.52	23.21	7.69	1.72	4.02	0.28
Dendrites	Average	60.79	23.52	7.80	1.81	4.03	0.35
	Max	60.92	23.78	8.01	1.89	4.05	0.38
	Min	58.16	23.51	8.61	2.78	3.60	0.40
Spaces	Average	58.62	23.63	8.96	3.11	3.68	0.55
	Max	59.81	23.80	9.23	4.02	3.92	0.60

(a) (b)
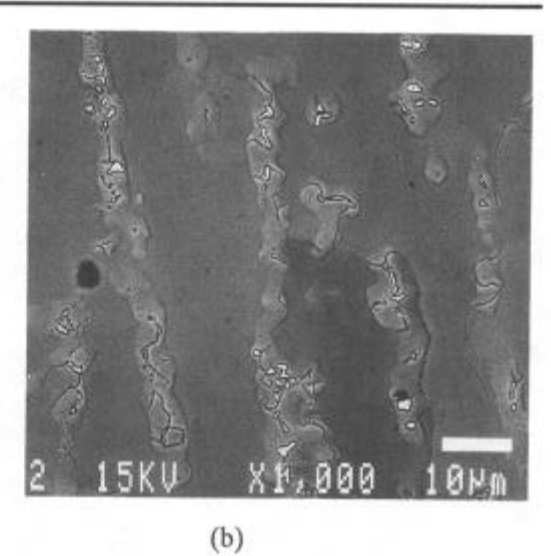
Figure 2- SEM micrographs of rough-weld a) secondary electrons b) back-scattered electrons.

In the rough-welded condition, the present minor phases in the interdendritic spaces have been identified, corresponding to Laves phases, MC and M_6C carbides (fig. 3). The typical chemical compositions of which are shown in table V. The Laves phases have a hexagonal structure and lattice parameters a = b = 0.47 nm, c = 0.74 nm, c/a = 1.58; the MC carbides (M = Nb, Mo, Ti) and the M_6C carbides (M = Ni, Nb, Mo, Cr, Si) have a face-centred cubic (fcc) structure and lattice parameters of 0.43 nm and 1.12 nm respectively. These results are in agreement with those of earlier studies conducted on weld alloy 625 (8,9).
The examinations on micrographic sections do not evidence any structural evolution between the rough-welded condition and treated conditions: 8 h at 600, 650, 700 and 750°C (Fig. 4).

Table V- Typical chemical compositions obtained on thin foils of the interdendritic phases in rough-welded condition (weight %)

Phases	Ni	Mo	Nb	Cr	Fe	Si	Ti
Laves	42.6	19.4	16.2	18.2	2.3	1.3	-
MC	1.7	9.9	81	2.7	-	-	4.7
M_6C	29.7	26.1	25	14.7	1.6	2.9	-

The TEM examinations on thin foils show the presence, as from 700°C, of ordered platelets featuring a body-centred tetragonal intermetallic metastable γ" Ni_3Nb phase, finely scattered within the matrix in the vicinity of the interdendritic phases, and conferring a speckeled appearance to the structure (Fig. 5). The platelets featuring lattice parameters a = b = 0.37 nm, c = 0.734 nm have developed in the three basic directions of the face-centred cubic matrix, resulting in three γ" orientations (Figure 5). In the "as-treated" condition after 8 h heat
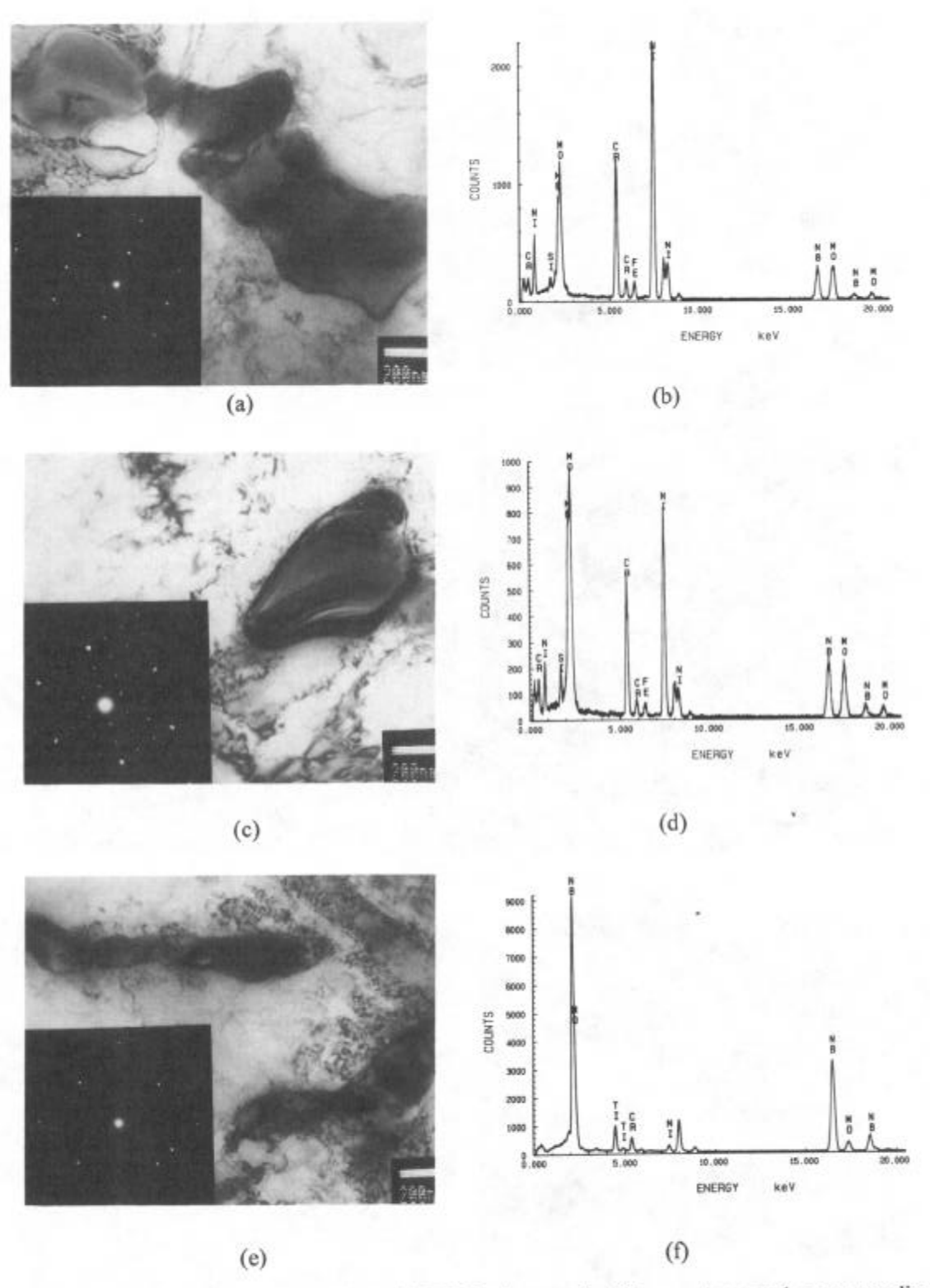
(a)

(b)

(c)

(d)

(e)

(f)

Figure 3 - Rough-welded condition - (a) TEM micrograph of Laves phase and corresponding [1$\bar{1}$00] selected area diffraction pattern (SADP) - (b) Laves phases X-EDS spectrum - (c) TEM micrograph of M_6C carbides and corresponding [1$\bar{1}$0] SADP - (d) M_6C carbides X-EDS spectrum - (e) TEM micrograph of MC carbides and corresponding [001] SADP - (f) MC carbides X-EDS spectrum.
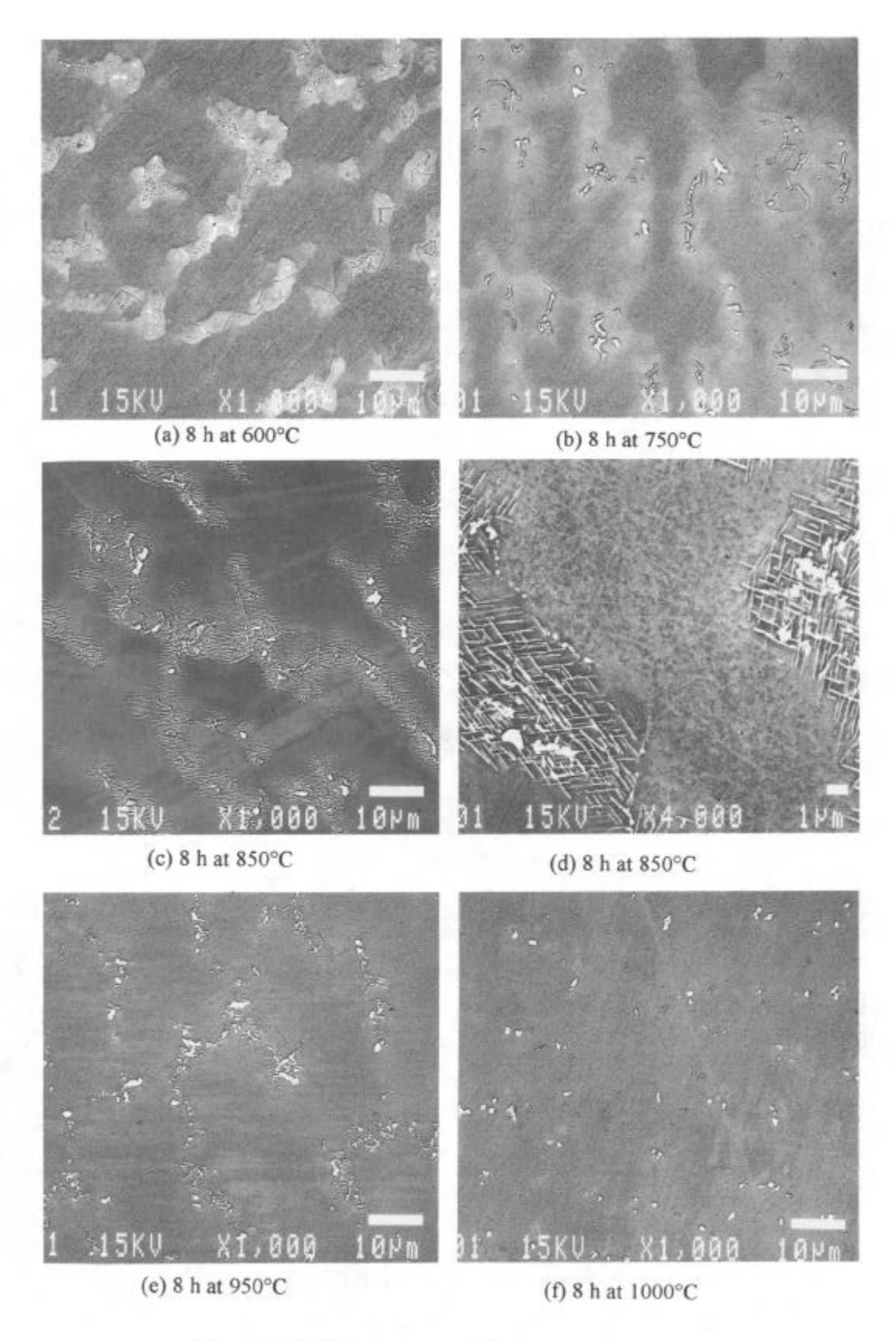
863

(a) 8 h at 600°C

(b) 8 h at 750°C

(c) 8 h at 850°C

(d) 8 h at 850°C

(e) 8 h at 950°C

(f) 8 h at 1000°C

Figure 4 - SEM back-scattered electron micrographs.

treatment at 750°C, the γ" phase precipitates are no longer exclusively distributed in the matrix, but also on the dislocations and slip bands, and this more particularly in the vicinity of the massic interdendritic phases, generating dislocations during the cooling process: Laves phases especially. The 8 h heat treatments at 850 and 950°C cause precipitation, in the interdendritic spaces, of a needle-shaped phase which may reach 5 μm (Fig. 4c to e). The TEM examinations show that, for the said temperatures, the γ" phase precipitates have disappeared, and that the orthorhombic stable intermetallic δ Ni_3(Nb, Mo, Cr, Fe, Ti) phase has appeared, featuring a lattice parameter a = 0.51 nm, b = 0.43 nm and c = 0.45 nm (Fig. 6). The typical composition of δ phase needles extracted on replicas (weight %) is: Ni = 55.7, Nb = 25.5, Mo = 12.6, Cr = 3.5, Fe = 1.8, Ti = 0.9. As from 850°C, fine M_6C (M=Mo, Ni, Cr, Nb, Si) carbides appear in the grain boundaries, of a size less than 0.2 μm. They are nucleated separately on both sides of the grain boundaries with coherent boundary on its matrix side.

After 8 h heat treatment at 1000°C, no difference exists in terms of atomic contrast images between the dendrite cores and the interdendritic spaces. The δ phase needles present in the interdendritic spaces at 850 and 950°C have disappeared (Fig. 4f), which is confirmed by the TEM examinations on thin foils. Precipitation of M_6C carbides has increased at grain boundaries.

Elementary segregations

Two types of elementary segregations are observed. The first relates to the γ primary dendrite cores, reflecting the chemical unbalance of the solidification. The second corresponds to the latest events of the solidification, resulting in Nb, Mo, Si over-saturation of the interdendritic spaces (Table IV) with precipitations of the Nb, Mo and Si rich minor phases, such as the Laves phases and the MC and M_6C carbides.
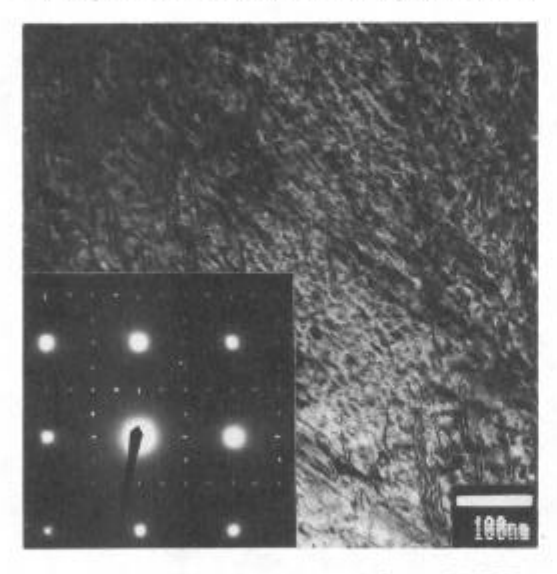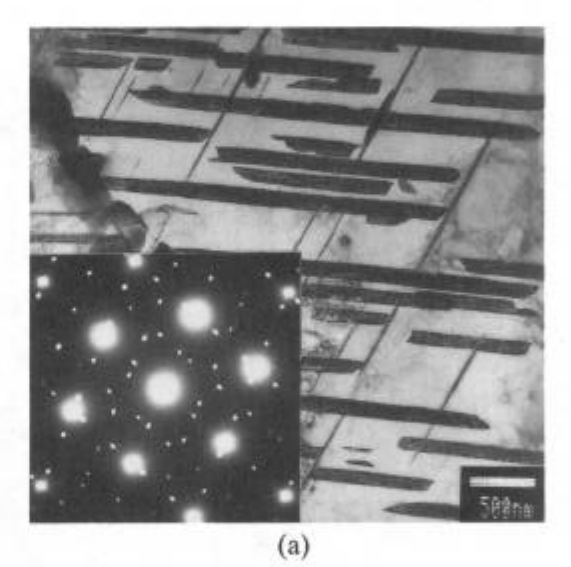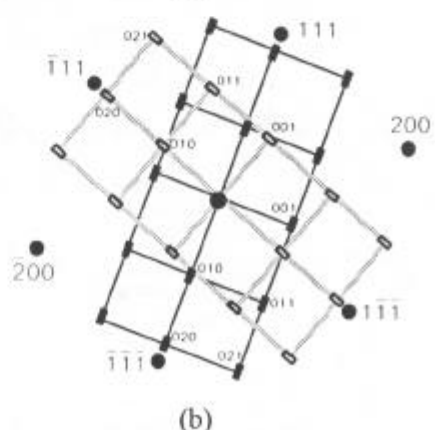

Figure 5 - Heat treatment 8 h at 700°C - TEM micrograph and [001] γ SAD pattern and family of the [100] [010] and [001] zones in γ".

Figure 6 - Heat treatment 8 h at 850°C - (a) TEM micrograph of δ needles and [0$\bar{1}$1] γ and [$\bar{1}$00] δ SAD pattern - (b) Corresponding indexing of the SAD pattern in (a).
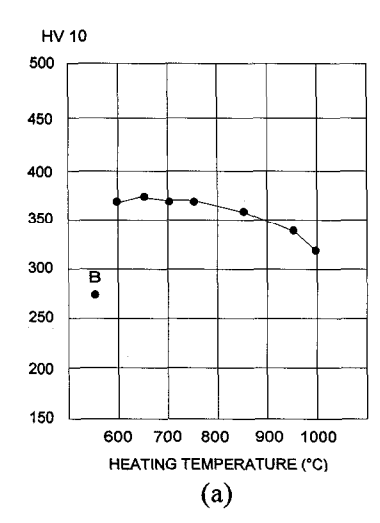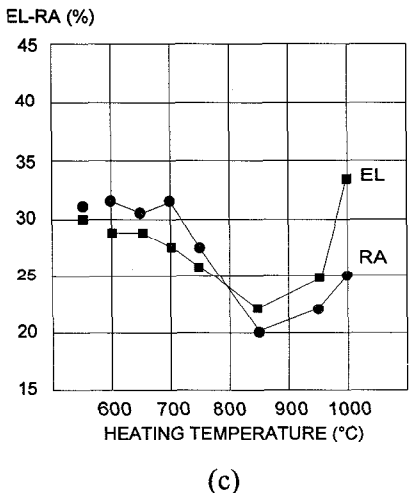

(a)

(b)

During the heat treatments, the heterogeneities vanish (Fig. 2b, 4 and 7). The average concentration ratios of the Nb, Mo, Si, Cr, Ni Fe elements between the interdendritic spaces and the dendrite cores, which feature but little evolution up to the temperature of 850°C, will tend toward 1 beyond the said temperature. The chemical composition heterogeneity between the dendrite cores and interdendritic spaces has practically disappeared after 8 h treatment at 1000°C.

Evolution of the mechanical characteristics

The YS and UTS pass by a maximum situated at 700°C for heat treatment temperatures less than or equal to 750°C, in correlation with a reduction of the ductility and impact strength (Figure 8).
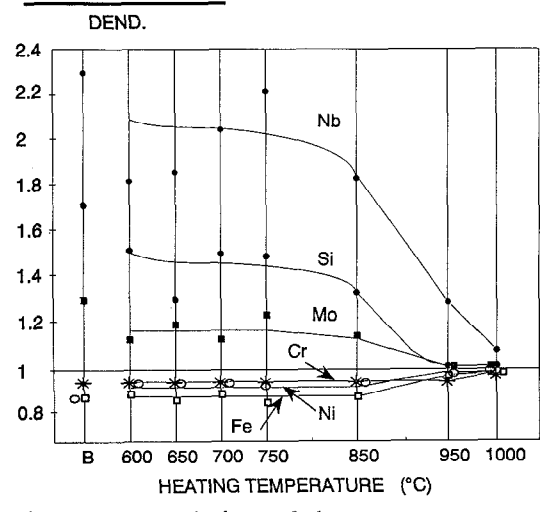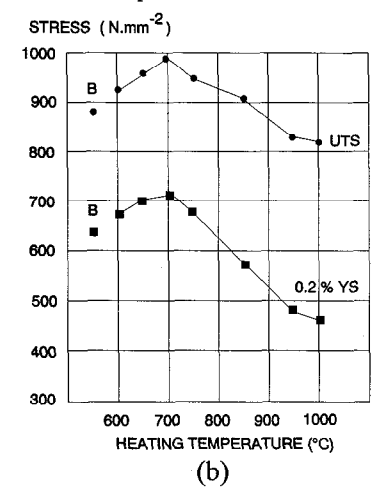
Figure 7 - Evolution of the average concentration ratios between dendrites cores and interdentritic spaces versus heat treatments.
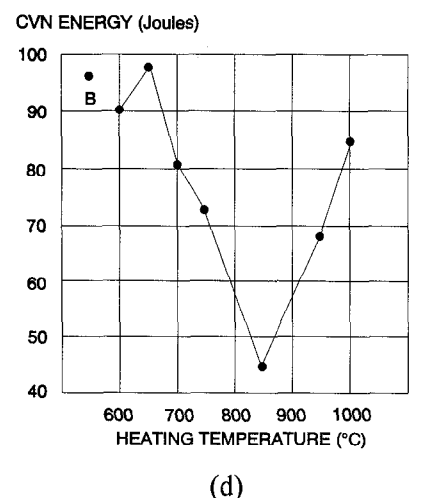
Figure 8 - Mechanical characteristics evolution vs heat treatments: (a) hardness, (b) UTS and YS, (c) ductility and (d) impact strength.

866

Compared with the rough-welded condition, the yield strength and UTS are respectively increased by 65 and 100 N.mm^{-2}. This increase of the mechanical strength and reduction of both the ductility and impact strength correspond to the precipitation field within the interdendritic spaces of the intermetallic γ'' phase , which is acknowledged as the principal strengthening source of alloy 625 (10,11).

A 8 h treatment at $750 < T < 950°C$ results in a reduction of all mechanical characteristics: mechanical strength, ductility, impact strength (Figure 8) in relation with the precipitation of the intermetallic δ phase needles in the interdentric spaces, the detrimental effects of which are known on the mechanichal strength and ductility of the superalloys that are precipitation strengthened by γ'' (10,12-14).

A 8 h heat treatment at 1000°C restores the ductility and impact strength characteristics further to δ phase dissolution (Figure 8). On the contrary, the higher the treatment temperature, the lower the mechanical strength, this being linked to the increased size of the grains which are no longer blocked by the precipitates.

Corrosion

Figure 9 shows the evolution of corrosion sensitivity during the ASTM G28 test, in terms of the treatment temperature. The SEM examination of the test specimens after the test shows that the weight losses are ascribable to the dissolution of the interdendritic spaces (Fig. 10). The most significant weight losses occur at the thermal states giving rise to significant interdendritic precipitations of γ'' phase for the treatment conditions at 700 and 750°C (Fig. 10a) and of δ phase for the treatment conditions at 850 and 950°C (Fig. 10b).
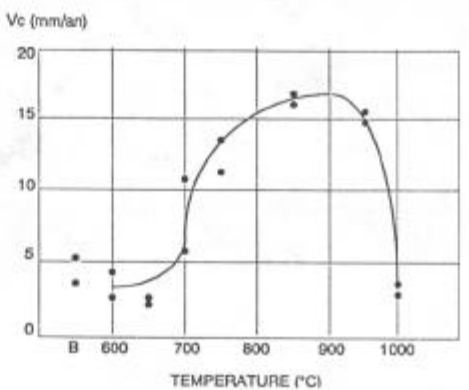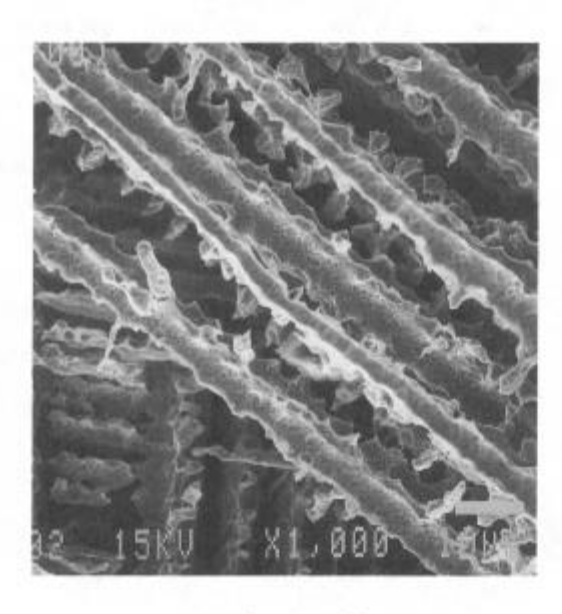

Figure 9 – ASTM G28 results .

The treatment conditions below 700°C and at 1000°C feature the lowest attacks, as the precipitations within the interdendritic spaces are not significant.
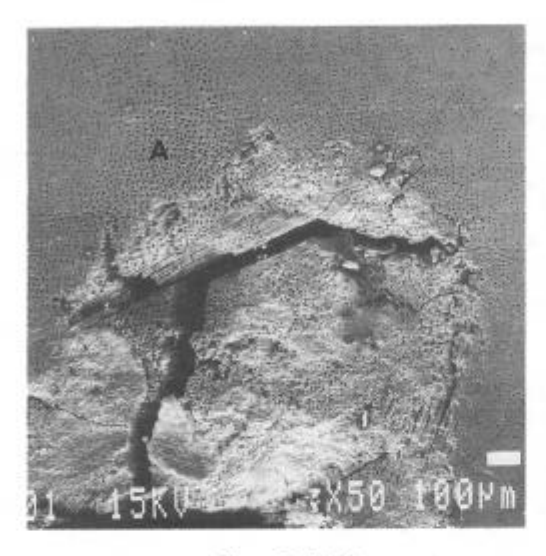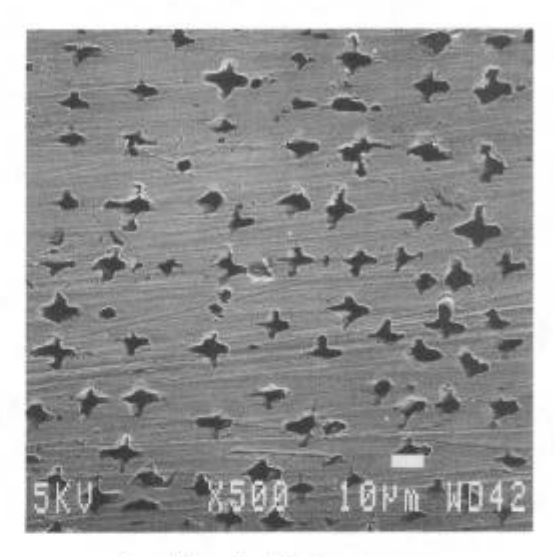

a - 8h at 700°C   b - 8h at 950°C

Figure 10 - SEM micrographs after ASTM G28 tests.

For ASTM G 48, irrespective of the thermal state of the material, no pitting appears up to a testing temperature of 90°C. At 95°C, all test specimens in rough-welded condition and

subjected to 8 h heat treatments between 600 and 850°C show significant interdendritic pits (Fig. 11) which may transform into cavities by dissolution of the interdendritic spaces (Fig. 11b). At 950 and 1000°C, rehomogeneisation of element contents between dendrites and interdendritic spaces is achieved, and the material is no longer sensitive to pitting.
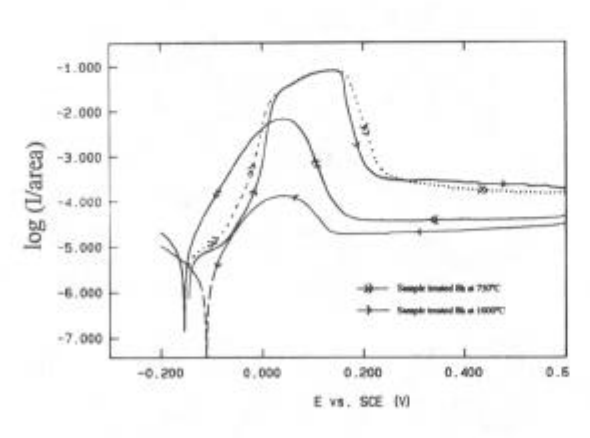

a- 8h at 750°C   b- A detail of (a)

Figure 11 - SEM micrographs after ASTM G48 test at 95°C.

Examples of reactivation charge curves obtained from two different thermal states are shown on Figure 12. Figure 13 shows the evolution of the C_a/C_p ratios in terms of the heat treatment temperature. The thermal states the most sensitive to corrosion under the said conditions are those treated between 650 and 850°C. Corrosion essentially affects the dendrites, and the grain and basalt boundaries (Fig. 14). In the interdendritic spaces, γ'' phase is more significantly attacked than δ phase, thus explaining that the highest corrosion rates are obtained for the heat treatments performed at 700 and 750°C. Above 950°, the C_a/C_p ratio decreases, and attacks are no longer present.
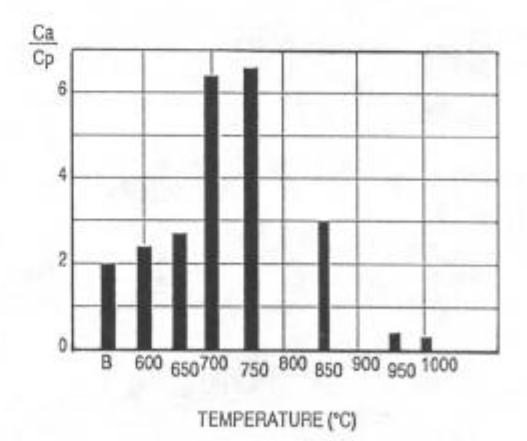

Figure 12 - Reactivation charge curves.   Figure 13 - Evolution of C_a/C_p ratio.

Irrespective of alloy thermal state, the current/potential curve in 30 g/l NaCl medium is identical (Fig. 15). It features a wide passivation step, without field of activity up to 600 mV/ECS. A secondary activity peak appears around + 800 mV/ECS, transpassivity having no effects below + 1.2 V/ECS. This behaviour is the indication of a definitely stable passivity, and total insensitivity to pitting.
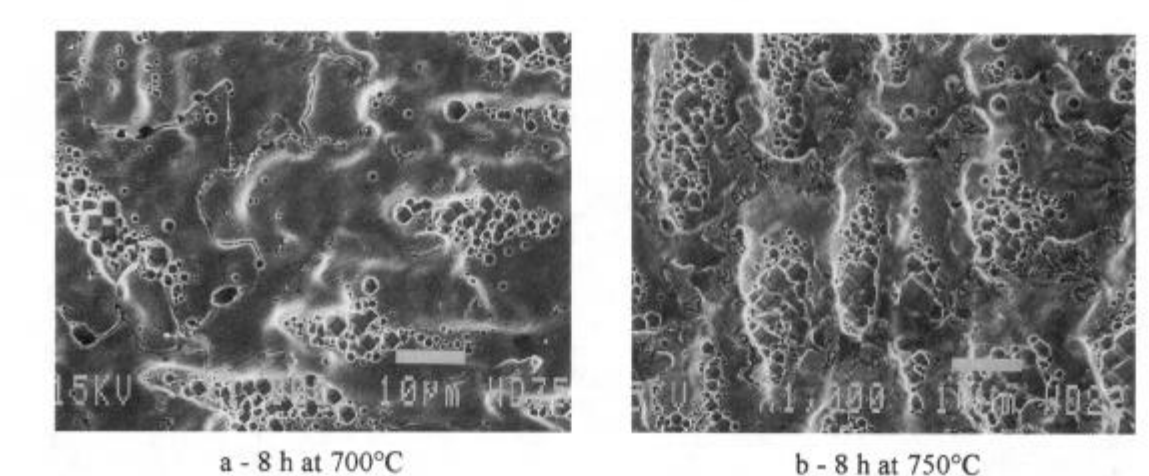
| a - 8 h at 700°C | b - 8 h at 750°C |

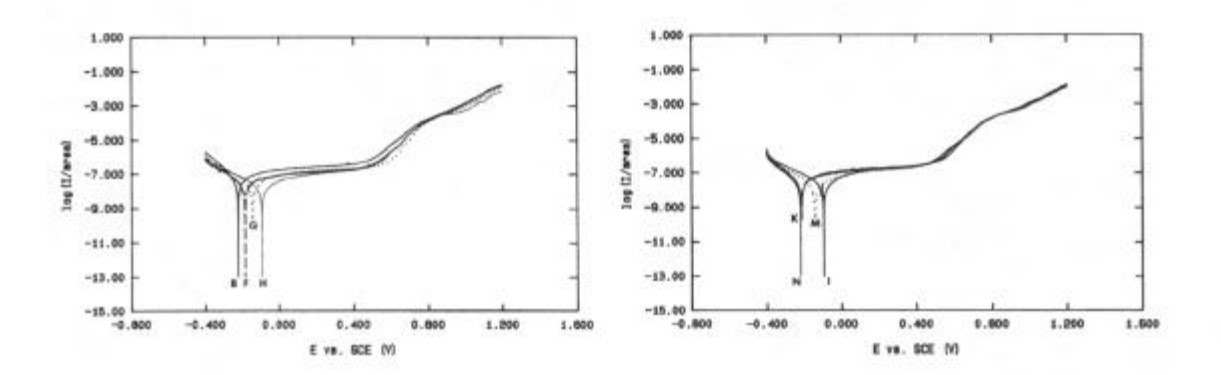Figure 14 - SEM micrographs after reactivation charge test.

Figure 15 - Intensity/potential curves in NaCl 30 g/l

Discussion

The structural and mechanical characteristics of the material in the rough-welded condition are in agreement with the results given in the litterature (7-9,11). Concerning the effects of short duration heat treatments of the industrial type (8 h) on the structure, the mechanical properties and corrosion resistance of weld alloy 625 on which few data is available, direct comparison between the behaviour of forged metal ("homogeneous") and weld alloy 625 ("heterogeneous"), without significant meaning apparently, is in fact particularly interesting from the industrial viewpoint. Indeed, in welded assemblies, both the parent and weld metals 625 may be present, and it seems important to know the heat treatment temperature ranges allowing not to impair the characteristics of both the parent and weld metals. The comparison of the results obtained in the same heat treatment conditions on forged metal 625 (4) of chemical composition similar to that of the weld metal under study shows, on the one hand, that precipitation of the δ phase not observed in the case of forged metal 625, "homogeneous" material, occurs in the case of weld alloy 625, "heterogeneous" material, for 8 h temperature hold times at temperatures in excess of 750°C and less than 850°C, with catastrophic effect on the mechanical characteristics and, on the other hand, that the heat treatments below 650°C and above 1000°C are the sole treatments allowing to prevent embrittlement and impairement of corrosion resistance of alloy 625.

Conclusions

Alloy 625, which combines good mechanical strength and good corrosion resistance concurrently with good weldability characteristics, can be used for welding low alloyed or high

strength steels with alloy 625, for repairing them by welding process, or coating them for corrosion protection purposes. In such cases, post-welding heat treatments are necessary, which must neither alter the charateristics of weld alloy 625, nor those of the parent metal 625 when the latter is also present in the welded joint. The effects of industrial type heat treatments: 8 h hold times at temperatures comprised between 600°C and 1000°C, on the structural, mechanical and corrosion resistance characteristics of weld alloy 625 has been studied. During the heat treatments, the mean concentration ratios of Nb, Mo, Si, Cr, Ni and Fe elements between the interdendritic spaces and dendrite cores feature but little evolution up to 850°C. Beyond that temperature, this ratio tends towards 1, and it can be observed that the weld metal composition heterogeneity has practically disappeared at 1000°C. A 8 h heat treatment at temperatures comprised between 650°C and 750°C results in increased mechanical strength values and decreasing ductility and impact strength linked to the precipitation of the body-centred tetragonal intermetallic γ'' Ni$_3$Nb phase in the interdendritic spaces. A 8 h heat treatment in the temperature range comprised between 750°C and 950°C has a catastrophic effect on all mechanical characteristics, in relation with the precipitation, in the interdendritic spaces, of the orthorhombic stable intermetallic δ phase Ni$_3$(Nb, Mo, Cr, Fe, Ti). At 1000°C, the ductility and impact strength are restored. However, the higher the heat treatment temperature, the lower the mechanical strength. The heat treatments have no effect on pitting resistance of weld alloy 625 in sea-water environment. The comparison of the results of this study with those obtained during a similar study conducted on forged metal 625 of comparable chemical composition subjected to the same heat treatments shows that heat treatments below 650°C and above 1000°C are the sole processes enabling to avoid embrittlement and impairment of the corrosion resistance of alloy 625.

Acknowledgements

References

1. S. C. HAYES : Report DE81030005, G. E. C. Knolls Atomic Power Laboratory, Schenectady, NY, September 1981.
2. J. P. HAMMOND : ASME Winter Annual Meeting on Ductility and Toughness Considerations in Elevated Temperature Service, San Francisco, December 1978, ASME MPC8, 63-67.
3. K. KROMPHOLTZ, R. TIPPING and G. UHLRICH :Z. Werkstofftech, vol. 15, 1984, 199-206.
4. C. VERNOT-LOIER and F. CORTIAL : Superalloys 718, 625 and Various Derivatives, E. Loria, Ed., TMS, Warrendale, PA, June 1991, 409-422.
5. G. CLIFF and G. W. LORIMER : J. Microsc., vol. 103, 1975, 203-207.
6. J. M. CORRIEU and C. VERNOT-LOIER : this volume.
7. M. J. CIESLAK, G. A. KNOROVSKY, T. J. HEADLEY and A. D. ROMIG Jr. : Metall. Trans. A, vol. 17A, 1986, 2107-2116.
8. M. J. CIESLAK, T. J. HEADLEY, T. KOLLIE and A. D. ROMIG Jr. : Metall. Trans. A, vol. 19A, 1988, 2319-2331.
9. M. J. CIESLAK : Welding Research Supplement, 1991, 49-56.
10. D. R. MUZYKA : The Superalloys, C. T. Sims and W. C. Hagel, eds., John Wiley, New York, NY, 1972, 113-143.
11. M. J. CIESLAK, T. J. HEADLEY and R. B. FRANK : Welding Research Supplement, 1989, 473-482.
12. J. F. BARKER, E. W. ROSS and J. F. RADAVICH : J. of Metals, 1970, 31.
13. G. E. KORTH and C. L. TRYBUS : Superalloys 718, 625 and Various Derivatives, E. Loria, Ed., TMS, Warrendale, PA, June 1991, 437-446.
14. R. COZAR, M. ROUBY, B. MAYONOBE and C. MORIZOY : Superalloys 718, 625 and Various Derivatives, E. Loria, Ed., TMS, Warrendale, PA, June 1991 423-436.